



Optimum Design of Piled Spill-through Bridge Abutment

Ahmed Khalaf ^{1*}, Adel Akel ², Osman Ramadan³

Abstract

The seismic behavior of spill-through bridge abutments is investigated under static load scenarios. This paper focuses on the performance of spill-through bridge abutments and aims at providing a framework for their seismic analysis and design. To do this, an extensive parametric study is conducted utilizing the FLAC[1] finite difference analysis tool. The examined parameters include cohesionless soils with variable strength; two different pile configurations; and three different types of soil slope profiles. Effects of these parameters on important system outputs are evaluated. The investigated system outputs cover pile axial forces and bending moments, depth of point of zero shear below ground surface, pile top displacement, and shear stresses in the surrounding soil. It is shown that the strength and deformation response of piles under earthquake loads are significantly affected by actual soil slope profile. Thus, this study encourages committees of design codes to modify their design methods of spill-through bridge abutment to include the support effects of soil.

Key Words: Pile group, Soil slope, Pile-slope system, Seismic behavior, Pseudo-static loads, FLAC

DOI Number: 10.14704/nq.2022.20.8.NQ44250

NeuroQuantology 2022; 20(8):2291-2311

2291

Introduction

In the field, pile foundations are often used to support constructions such as wharfs, bridges, and high-rise buildings. The main causes of lateral forces in piled bridge abutments are seismic movement of slopes, ground pressure, traffic movements, and braking. Laterally loaded piles should prevent geotechnical failure, structural failure and excessive deflections. The decks of traditional bridge abutments are supported by bearings, which are supposed to protect the deck from longitudinal forces caused by back fills, as well as the abutment wall from the effects of thermal deck expansion caused by daily and seasonal air temperature fluctuations. The so-called Spill-through abutment is another typical type of abutment. The abutment columns "piles" are embedded in the embankment that slopes down away from the cross beneath the bridge in this type of bridge abutment. Both the influence of soil in front of the abutment and the

effects of soil arching should be considered when designing a Spill-through abutment. In the literature, there are numerous research on the effect of inclined ground geometry on pile lateral response under static and dynamic loads (Chen 2001; Leavacher 1998; Wartman 2005) [2-4]. (Parkash and Kumar 1996)[5] developed method to predict load deflection relationship for single piles embedded in sand and subjected to lateral load, considering soil nonlinearity based on results of 14-full scale lateral pile load tests.

The majority of studies discovered in literature adhere to design codes, neglecting the fact that soil material is a structural element with stiffness that can affect soil pile interaction issues and just model it as a load. This study considers the effects of soil slope profiles and pile arrangement types on the analysis of spill-through abutments.

Corresponding author: Ahmed Khalaf

Address: ¹PhD Candidate ,faculty of Engineering, Cairo University ,Egypt, ²Professor of Structural Engineering, faculty of Engineering, Cairo University ,Egypt, ³Presently, Dean of Higher Technological Institute (HTI), 10th of Ramadan city, Egypt



Case Study Bridge Description

A multi-span continuous box girder bridge is the case study bridge. A fixed bot bearing attaches the deck to the end abutment. The Spill-through abutment is employed; abutment columns are embedded in the embankment in this style of structure. The interaction of soil structure with piled foundation Spill-through abutment is considered in this work. Case Study Bridge is classed as a semi-integral type with no expansion joints because the deck is attached to the abutment with a fixed bot bearing. Because of the bot bearing, the issues of moment continuity and rotation due to creep is no longer an issue. The structural stability of the soil embankment during strong motion is a seismic hazard concern in the construction of a pile-supported spill via semi-integral abutment bridge. In this study, numerical models based on the code FALC were used. This commercially available software uses the explicit finite difference approach to solve the entire equation of motion. It is capable

of doing a full dynamic ground response simulation. The unbounded nature of the dynamic soil structure system and the nonlinearity of the soil medium are two fundamental properties that distinguish it from other general dynamic structure systems. In the longitudinal direction, the bridge is idealized using a 2D plain strain model. Both the piled foundation and the deck are assumed to be linear elastic throughout the analysis, as is standard practice in design codes, while inelastic soil behavior is considered in the near slope zone, where the most inelastic behavior is expected, and near bed rock and boundaries, where model linear elastic soil behavior is accepted. A typical spill-through semi-integral abutment is supposed to be constructed on a uniform soil profile that extends to a full depth of 41.0 m above bedrock. As shown in the images, a 9.0 m high earth embankment with varying shapes and angles is supported by one or two rows of piles. Along the length of the abutment, each row of piles is spaced at 3.0 meters (3 times the pile diameter)

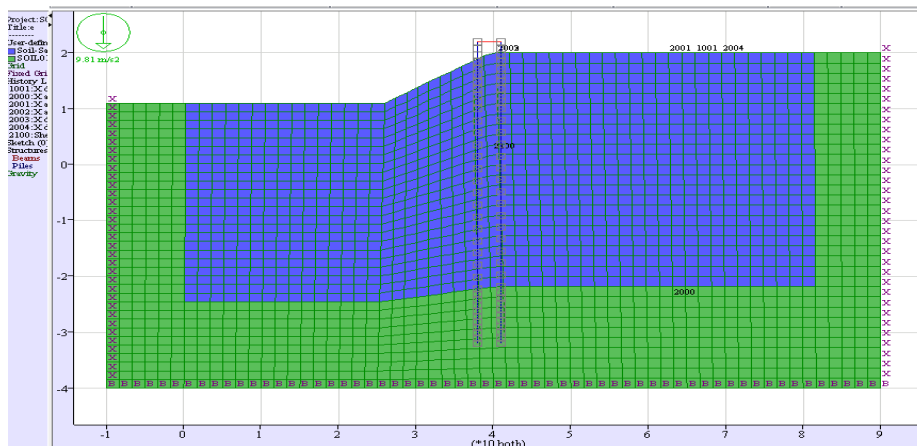


Fig. 1: Profile P1 (Two Rows of Pile Abutment & slope 3:2 without slope terrace)

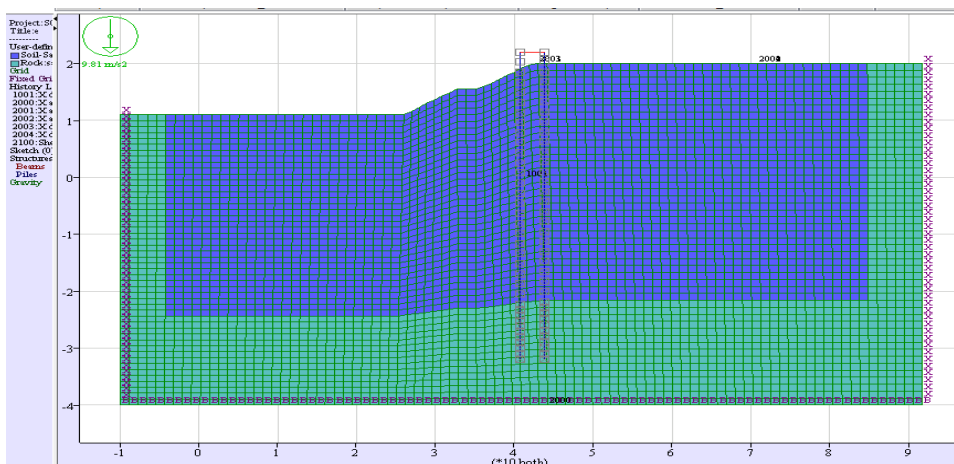


Fig. 2: Profile P2 (Two Rows of Pile Abutment & slope 3:2 with slope terrace)

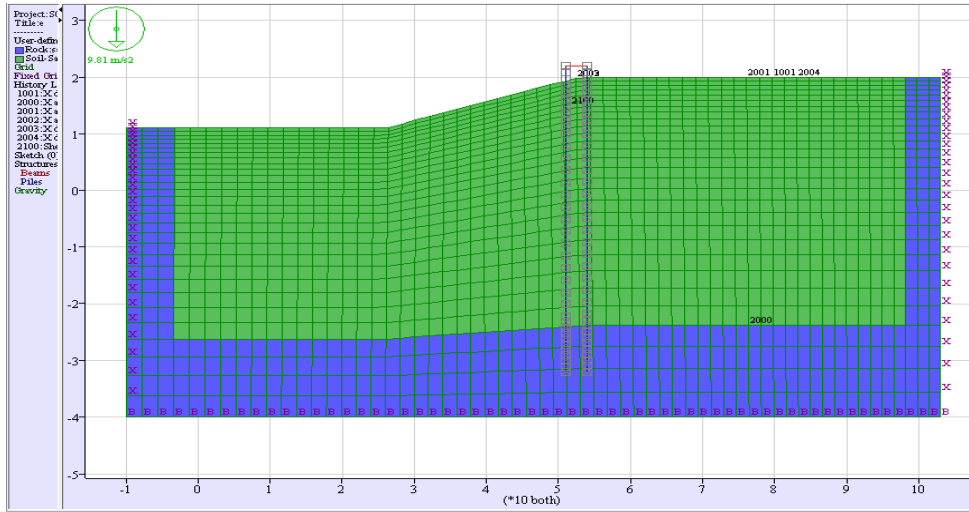


Fig. 3: Profile P3 (Two Rows of Pile Abutment & slope 3:1 without slope terrace)

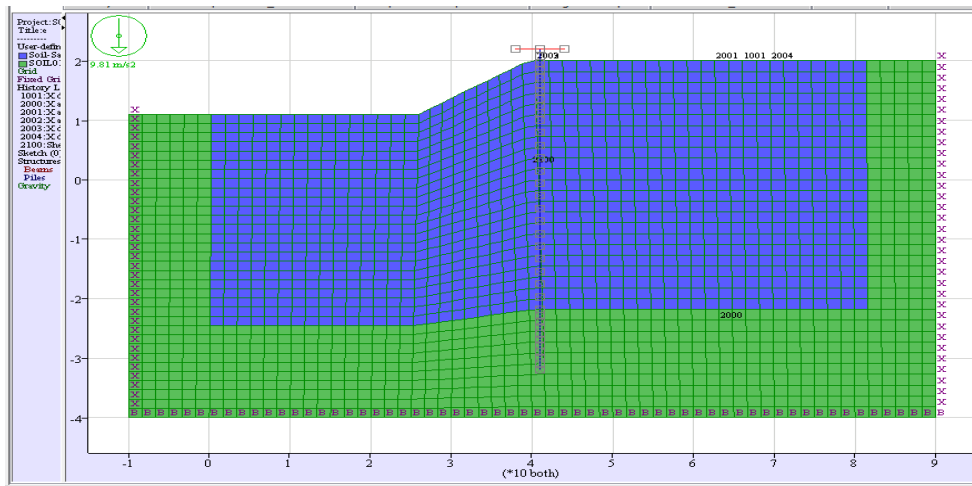


Fig. 4: Profile P4 (One Row of Pile Abutment & slope 3:2 without slope terrace)

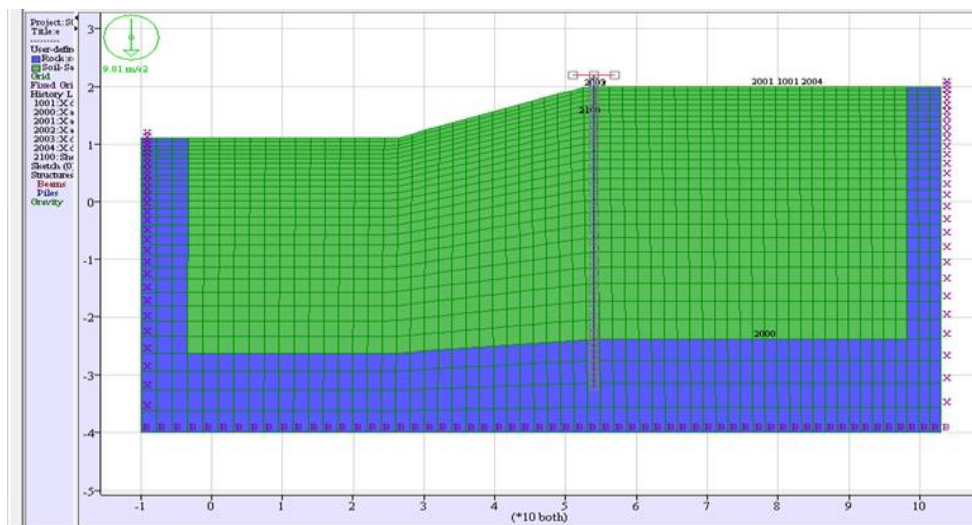


Fig. 5: Profile P5 (One Row of Pile Abutment & slope 3:1 without slope terrace)

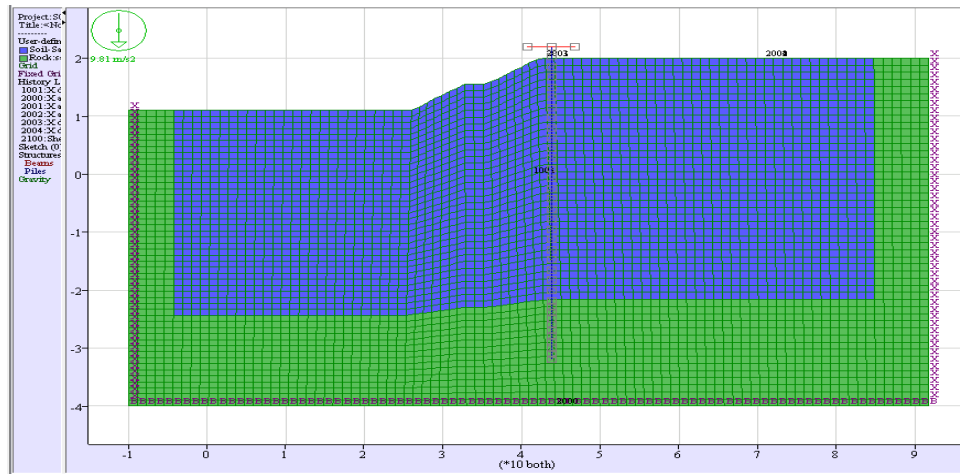


Fig. 6: Profile P6 (One Row of Pile Abutment & slope 3:2 with slope terrace)

The soil profile was modeled using elastic-plastic material and the Mohr-Coulomb failure model, with the material behaving elastically until yielding. Hysteretic soil behavior allows for a drop-in shear

modulus with strain level in the dynamic analysis reported in the second portion of the research. The following table lists the material qualities of soil and bedrock

Table 1: Drained properties for Soils and Rock

Soil Parameters	Soil D	Soil C	Soil B
Dry density (kg/m ³)	1800	20000	2200
Shear modulus (MPa)	25.92	265	828
Poisson's ratio	0.3	0.3	0.3
Cohesion (MPa)	0	0	0
VS(m/sec)	120	360	600
Friction angle (degrees)	30	35	38

2294

Boundary condition

Boundary condition is the prescription of controlled condition along model boundaries. In static calculation, the bottom edge is fixed while the left and right boundaries were free to move vertically but fixed in horizontal direction. In dynamic analysis, the simulation of waves by finite difference method in unbounded domains requires a special treatment of lateral boundaries of the truncated computational domain. Quiet boundary by (Lysmer) involves dashpots attached independently to lateral boundary in normal and shear directions.

Interface element

The interface element is modeled as linear spring-slider system with interface shear strength defended by Mohr-Coulomb failure criterion. A recommended thumb rule according to FLAC manual is that normal and shear stiffness to be ten times equivalent stiffness of the stiffest neighboring zone in soil domain. By doing this, the deformability at the interface will have minimal influence on both

the compliance of the total model and the calculation speed

Static Analysis methodology

The nonlinear static analysis of soil-pile model proposed herein is divided into three phases to simulate the staged construction of the bridge
 Stage1: only soil embankment is modeled and the analysis is performed under own weight in order to develop the initial stress in the soil medium
 Stage2: the bridge structural elements are added and connected to soil medium, and the whole system is then analyzed using static analysis
 Stage3: Apply the static lateral load at top of system, without considering surcharge loads, and monitor the soil-pile system response

Parametric Study

The current research divided to two parts. first one of this paper, study the response of spill through



abutment to Quasi static lateral loads as a percentage of seismic weight applied at top level of abutment, sample of output graphs from FLAC software is present which include shear force,

bending moment, axial force of piles and lateral displacement of both piles and surrounding soil as shown in figure A

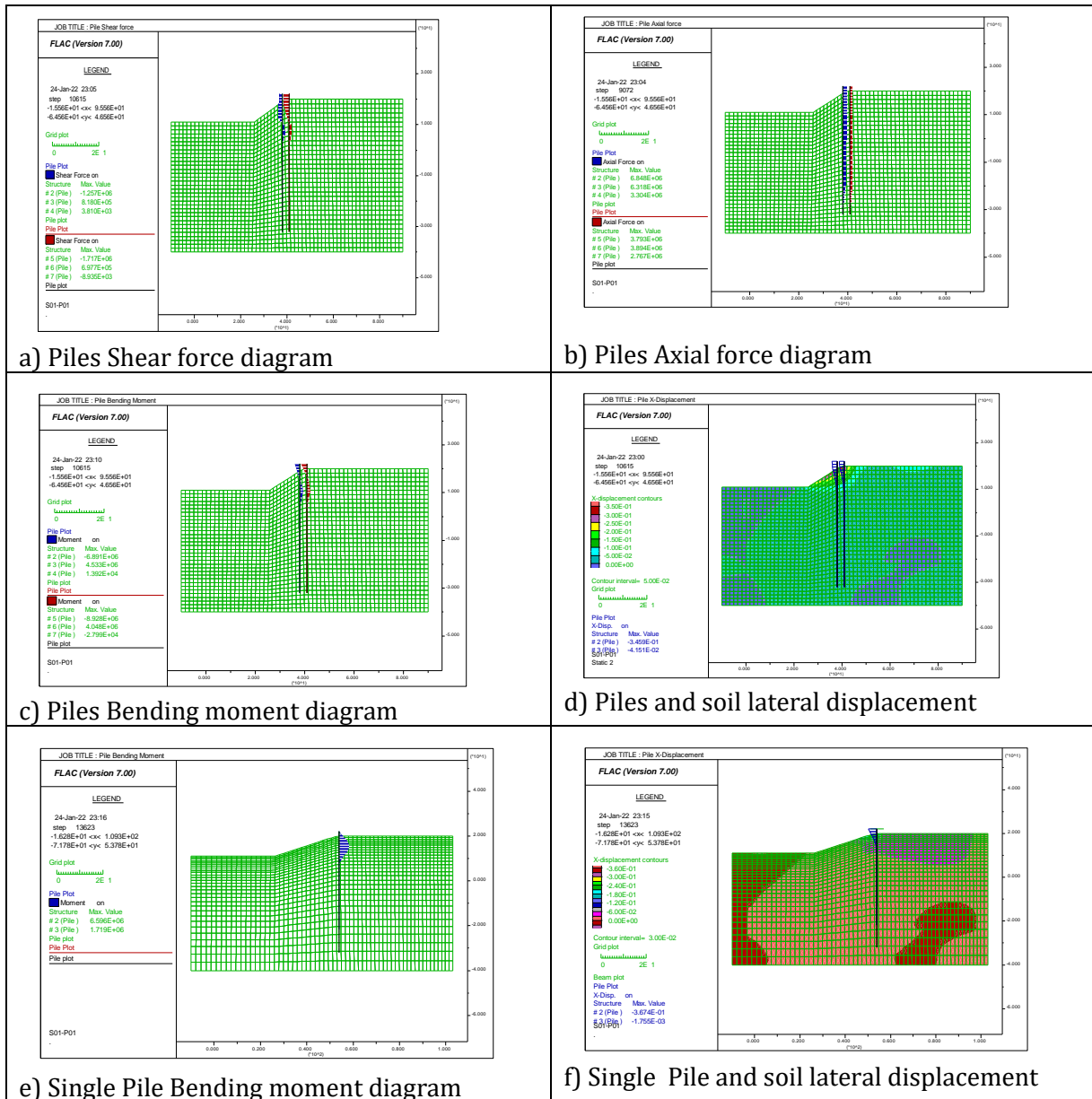


Fig. A: Sample of FLAC output graphs

Change in soil stiffness is used to analyze the effect of soil-pile interaction on the depth of point of zero shear as a percentage of slope depth (selected to be constant for all models 9.0 m). The depth of point of zero shear for near slope piles decreases with increased soil stiffness for models P1, P2, and P3 in figure 7, as supporting soil attracts lateral shear at shallow depth. The P2 profile with terrace point of zero shear is roughly 90% of the P1 profile for type

C&D soils, while the P3 profile with slope 3:1 is only 65%. In the case of soil type B, the P2 profile is 15% larger than the P1 profile at the terrace point of zero shear, with no change in zero shear depth between the P1 and P3 profiles. As seen in Figure 8, the depth of zero shear in far slope piles follows a similar pattern, with a minor drop in depth due to extra soil support in-between two rows of piles



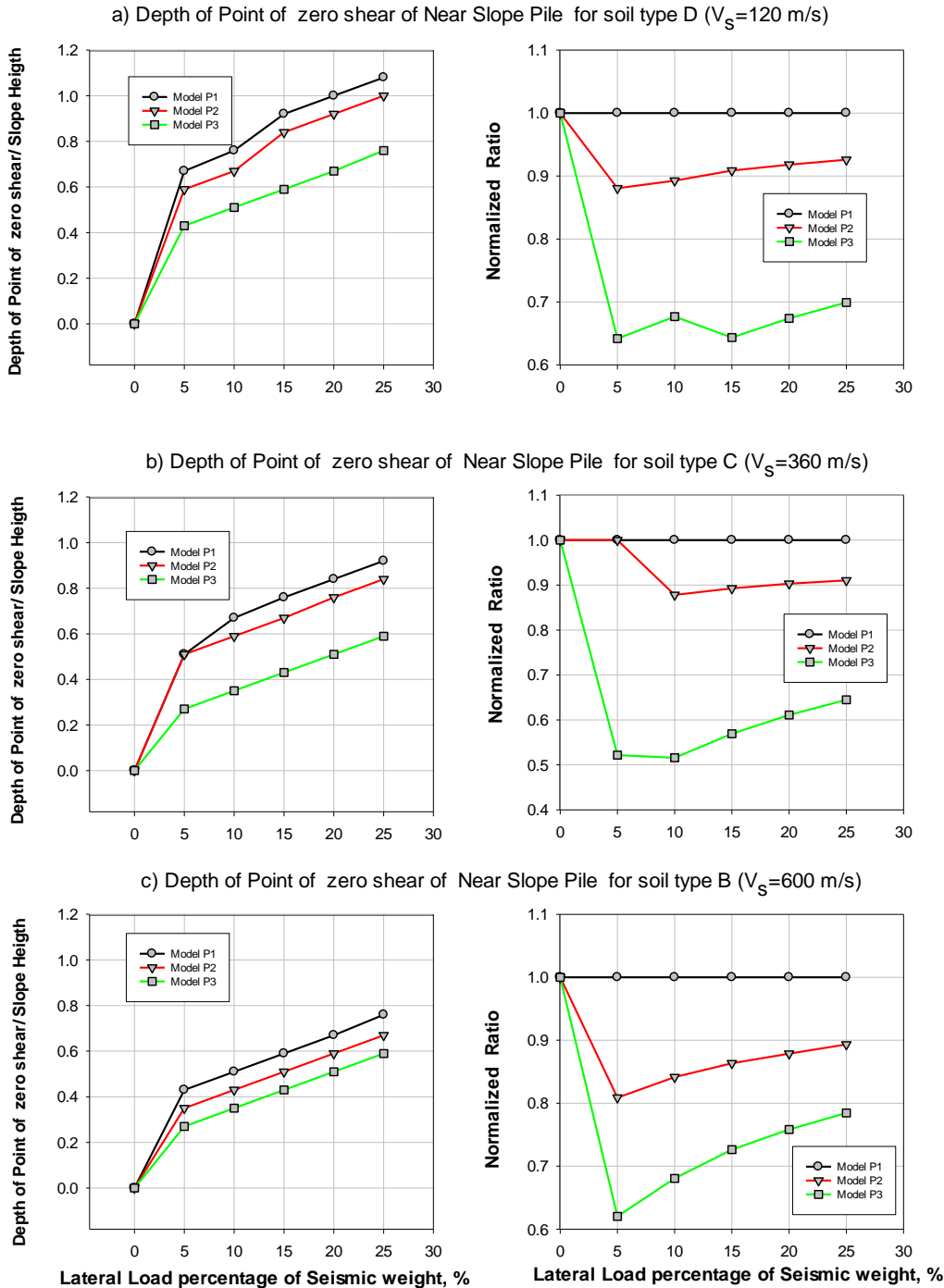


Fig.7: Normalized with respect to soil depth (9.0m) left figure and Normalized with respect to profile P1- right figure of point of zero shear for near slope piles versus lateral load coefficient a)for $V_s=120$ m/sec; b) for $V_s=360$ m/sec; c) for $V_s=600$ m/sec



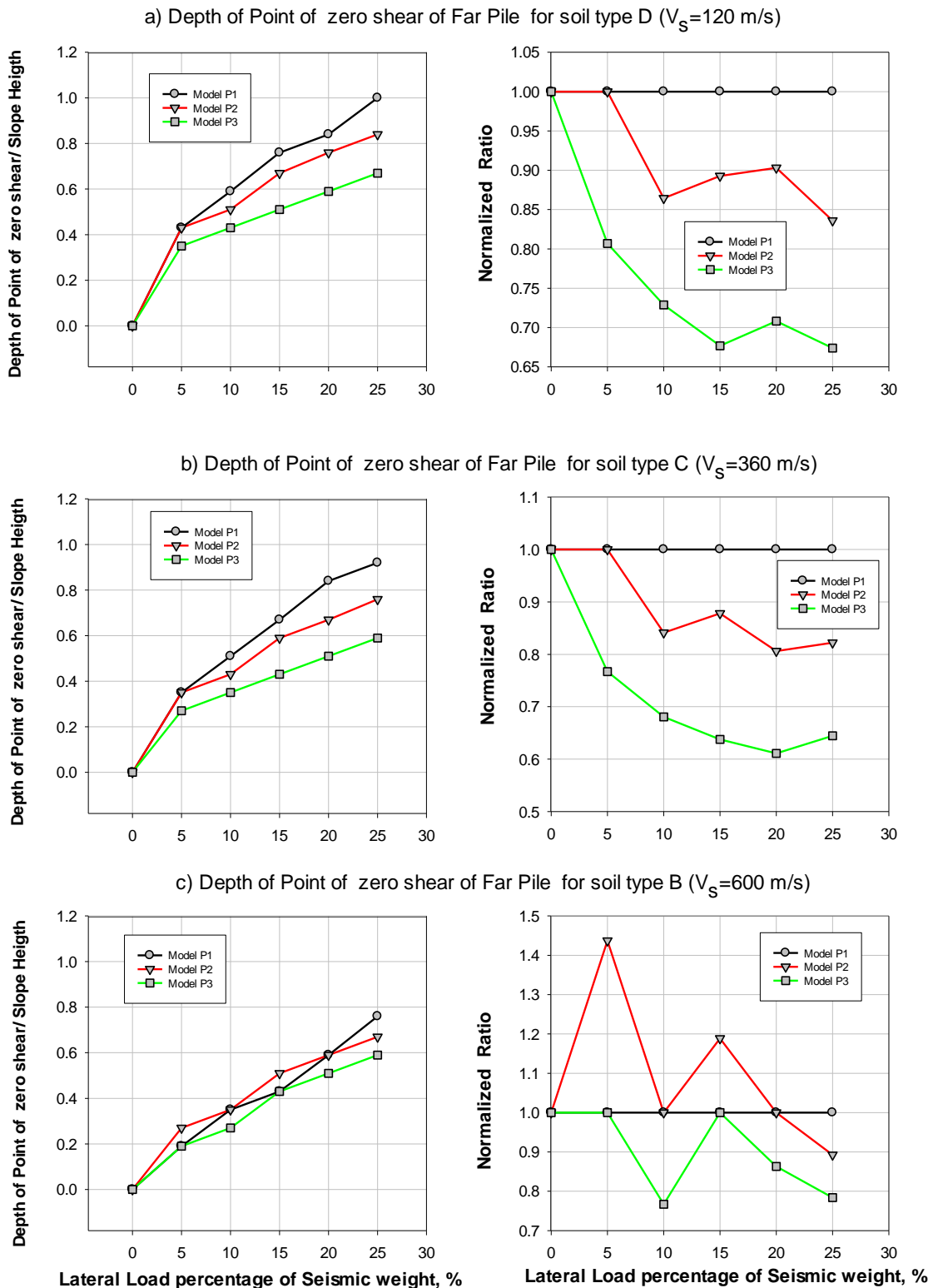


Fig.8: Normalized with respect to soil depth (9.0m) left figure and Normalized with respect to profile P1- right figure of point of zero shear for Far piles versus lateral load coefficient a)for Vs=120 m/sec; b) for Vs=360 m/sec; c) for Vs=600 m/sec

For models P4, P5, and P6 of a single row of piles, the lowest depth of zero shear of about 60% of the soil stiffness has a minor effect on the depth of zero shear, as shown in figure 9, implying that supporting soil attracts lateral shear at a shallow

depth in gentle slopes. One of the most significant characteristics to consider while considering the Spill through Abutments system is pile drift. The effect of slope shape and soil stiffness on lateral drift response is judged using the SEACO (Seismic design manual

2000)][6] recommended pile drift performance limit state. It's worth noting that the collapse limit state was examined using nonlinear static analysis, with deck drifts ratios derived based on pile free length measured from the slope's bottom level

Table 3: Deck drift various damage limit states as defined in SEAOC 2000 (Structural Engineering Association of California, seismic design manual)

Damage Scale Definition (Limit States)	Damage description	Deck Drift (mm %)	
		Longitudinal Direction	Transverse Direction
Fully Operational	Negligible	< 0.2	< 0.5
Operational (LS-1)	Minor local yielding at some piers may occur. No observable fractures. Minor buckling or observable permanent distortion of the bridge Members.	0.2 to 0.5	0.5 to 1.0
Life safety (LS-2)	Hinges form. Local buckling of some elements. Severe joint distortion. Isolated Connection failures. A few elements may experience fracture.	0.5 to 1.5	1.0 to 3.5
Near Collapse	Extensive distortion for the structure components and pier panels. Many fractures in connections.	1.5 to 2.5	3.5 to 5.0
Complete Collapse (LS-3)	-	> 2.5	> 5.0



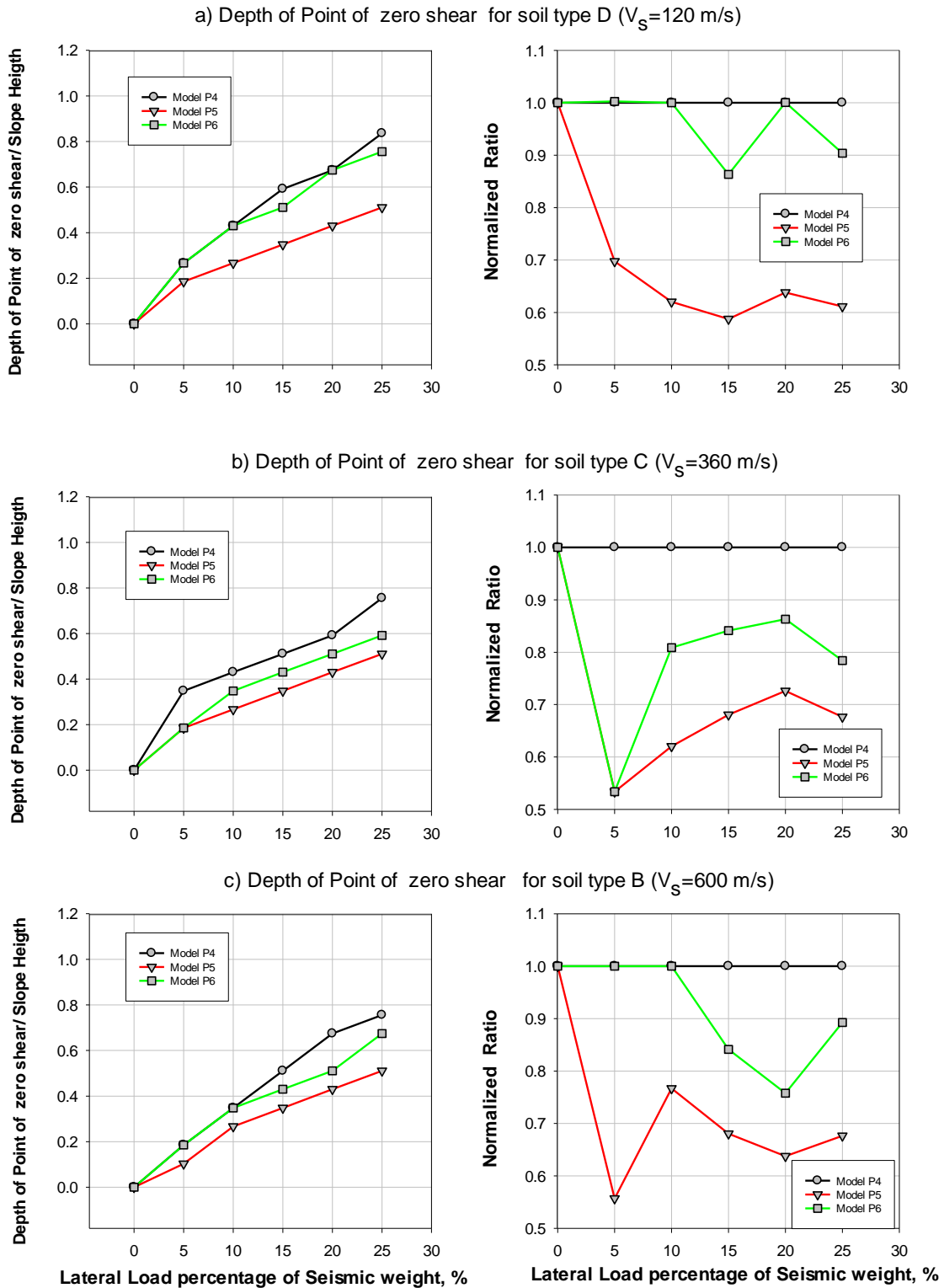


Fig.9: Normalized with respect to soil depth (9.0m) left figure and Normalized with respect to profile P4- right figure of point of zero shear for Single pile versus lateral load coefficient a)for $V_s=120$ m/sec; b) for $V_s=360$ m/sec; c) for $V_s=600$ m/sec

Increased soil stiffness clearly decreases drift and improves the performance of the pile-soil system for slope systems P1, P2, and P3 of two rows of piling systems depicted in figure 10. At a lateral load

intensity of around 20% of seismic weight, system P1 reaches a collapse limit state of drift ratio equal to 2.50 % ($\delta\theta=2.50$ %) for soil type D (weak soil). At a lateral load intensity of around 23% of seismic



weight, system P2 reaches its collapse limit condition. System P3, on the other hand, with a slope of 3:1, achieves a Life safety limit state of drift ratio of 1.50 % ($\delta\theta=1.50\%$) at a lateral load intensity of around 23 percent of seismic weight, indicating an improvement in response when compared to other systems. All studied systems do not approach the collapse limit state for soil type C (Medium soil) up to lateral load intensity of around 25% of seismic weight. At a lateral load intensity of around 19 percent of seismic weight, System P1 reaches the Life safety limit condition of drift ratio equal to 1.50 % ($\delta\theta=1.50\%$). At a lateral stress intensity of around 22% of seismic weight, system P2 reaches the Life safety limit condition. On the other hand, at a lateral

load intensity of roughly 18 percent of seismic weight, system P3 with slope 3:1 achieves an operational limit state of drift ratio equal to 0.50 % ($\delta\theta=0.50\%$). For soil type B (Strong soil), response of all systems is nearly equal with drift reach Operational limit state at lateral load intensity of about 16% to 19% of seismic weight.

For slope systems P4, P5, and P6 of single rows of piling systems shown in figure 11, increased soil stiffness has little effect on pile drift. The slope geometry, on the other hand, has a big influence on pile drift reaction. Drifts in system P5, which has a slope of 3:1, are about half of what they are in other systems



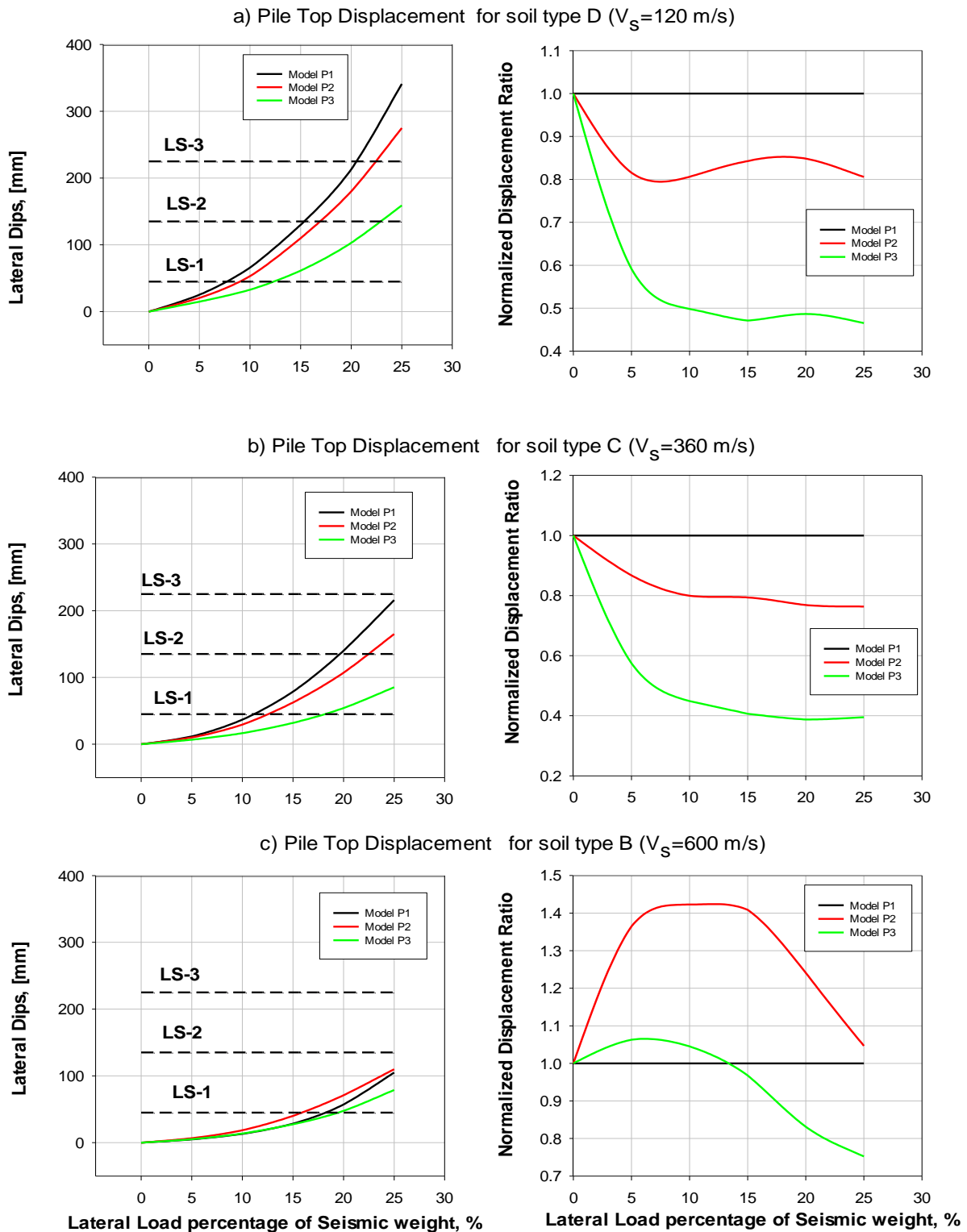


Fig.10: Lateral drift of two rows of piles systems left figure and Normalized with respect to profile P1- right figure versus lateral load coefficient a)for $V_s=120$ m/sec; b) for $V_s=360$ m/sec; c) for $V_s=600$ m/sec



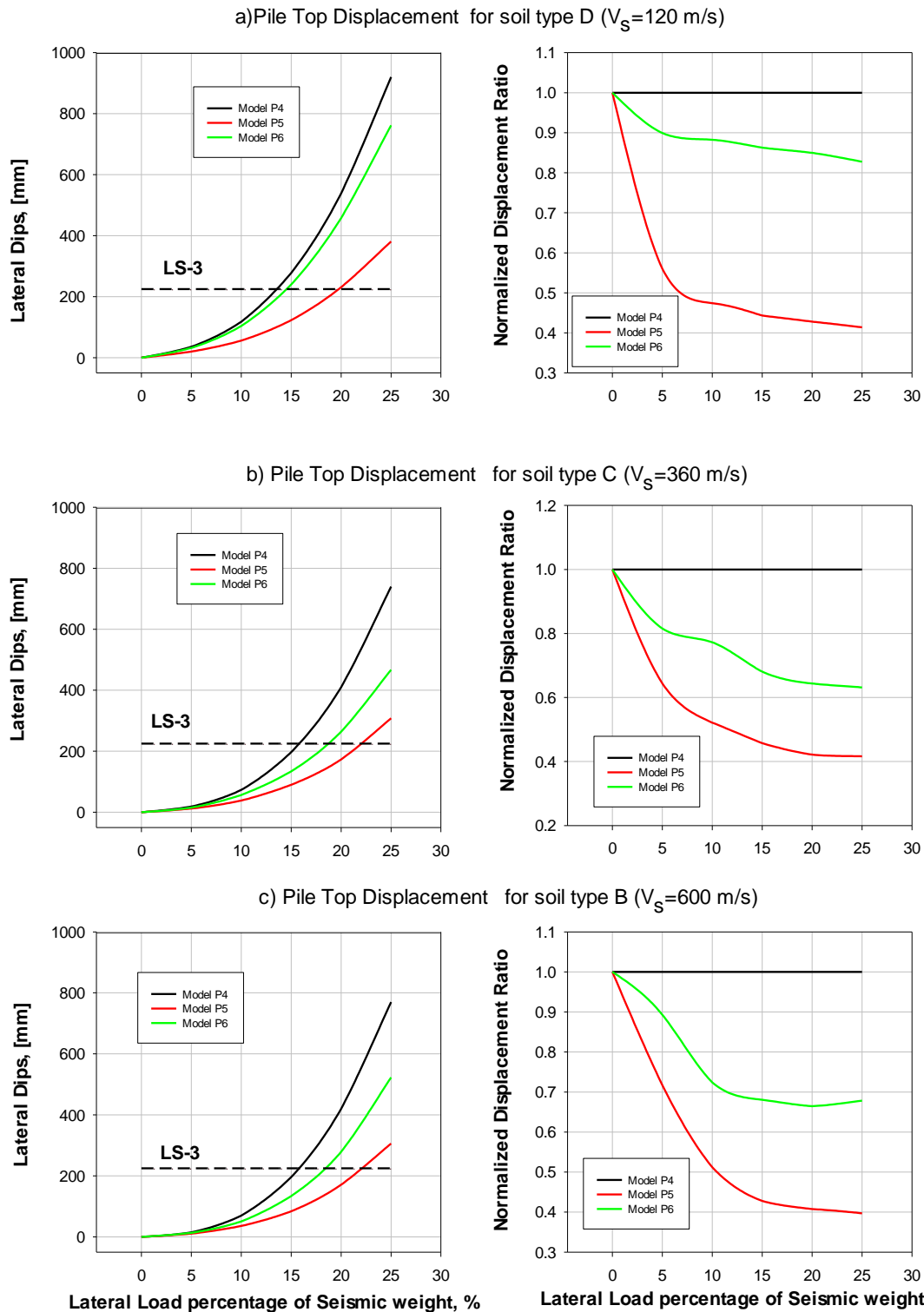


Fig.11 Lateral drift of Single row of piles systems left figure and Normalized with respect to profile P4- right figure versus lateral load coefficient a)for $V_s=120$ m/sec; b) for $V_s=360$ m/sec; c) for $V_s=600$ m/sec



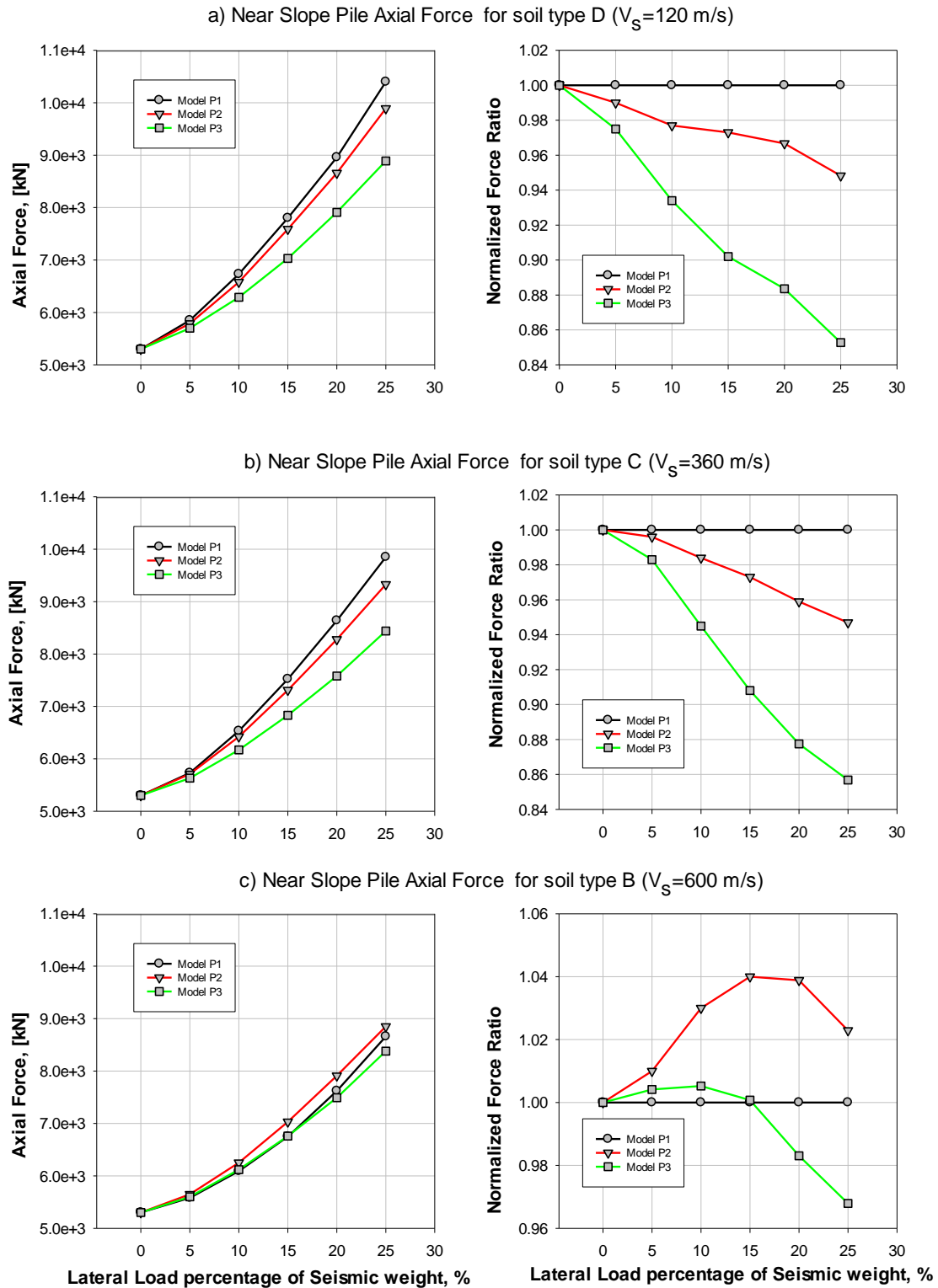


Fig.12: Axial force of near slope piles systems left figure and Normalized with respect to profile P1- right figure versus lateral load coefficient a)for $V_s=120$ m/sec; b) for $V_s=360$ m/sec; c) for $V_s=600$ m/sec



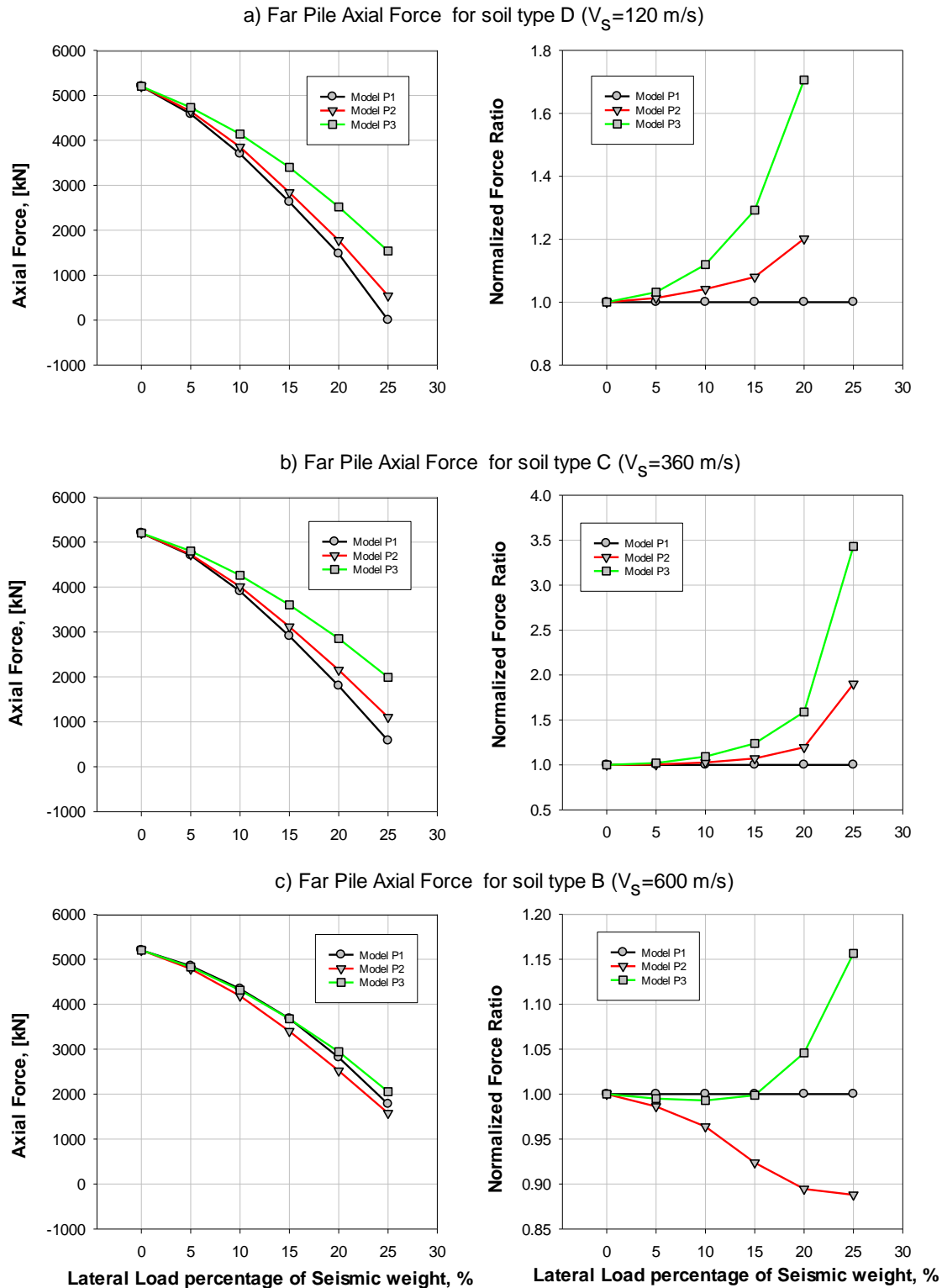


Fig.13: Axial force of Far piles systems left figure and Normalized with respect to profile P1- right figure versus lateral load coefficient a)for $V_s=120$ m/sec; b) for $V_s=360$ m/sec; c) for $V_s=600$ m/sec

As a common part of lateral load is communicated by axial force coupling in piles, the magnitude of axial force in both near slope and far pile in systems P1, P2, and P3 contains two rows of piles is greatly

affected by the magnitude of lateral load intensity. As demonstrated in figures 12 and 13, the magnitude of axial force is mostly controlled by the slope's form and the stiffness of the surrounding soil



Increase axial force inverse proportion to soil stiffness for near slope piles, as shown in figure 12. For both weak and medium soil, system P1 has the biggest increase in axial force, system P2 has a slight increase in axial force, and system P3 has the lowest increase in axial force. At strong soil, this phenomenon is less observable (type B soil).

As shown in Figure 13 for axial force in far piles, the decrease in pile axial force is inversely proportional to soil stiffness. For both weak and medium soil, the increase in axial force in the near slope pile is less than the decrease in axial force in the distant pile in systems P1 and P2. While the axial force near the slope is higher in system P3, this indicates that the slope's form supports the far pile and adds to the coupling force. On the other hand, systems P1 and

P2 soil increase coupling force for both weak and medium soil. All systems with strong soil (type B) exhibit a greater increase in near-slope axial force than a decrease in far-slope axial force.

Increased soil stiffness has affected bending moments for near slope piles, whereas increased soil stiffness has considerably reduced bending moments for far slope piles. Increased soil stiffness reduces pile moment by around 50% in systems P1 and P2.

In significant lateral load intensity, as seen in Figure 18 systems P4, P5, and P6 with single pile Spill-through abutment soil stiffness have a small influence on pile bending moments, but increasing slope (example of system P5 with slope 3:1) reduces pile moment by 25%.



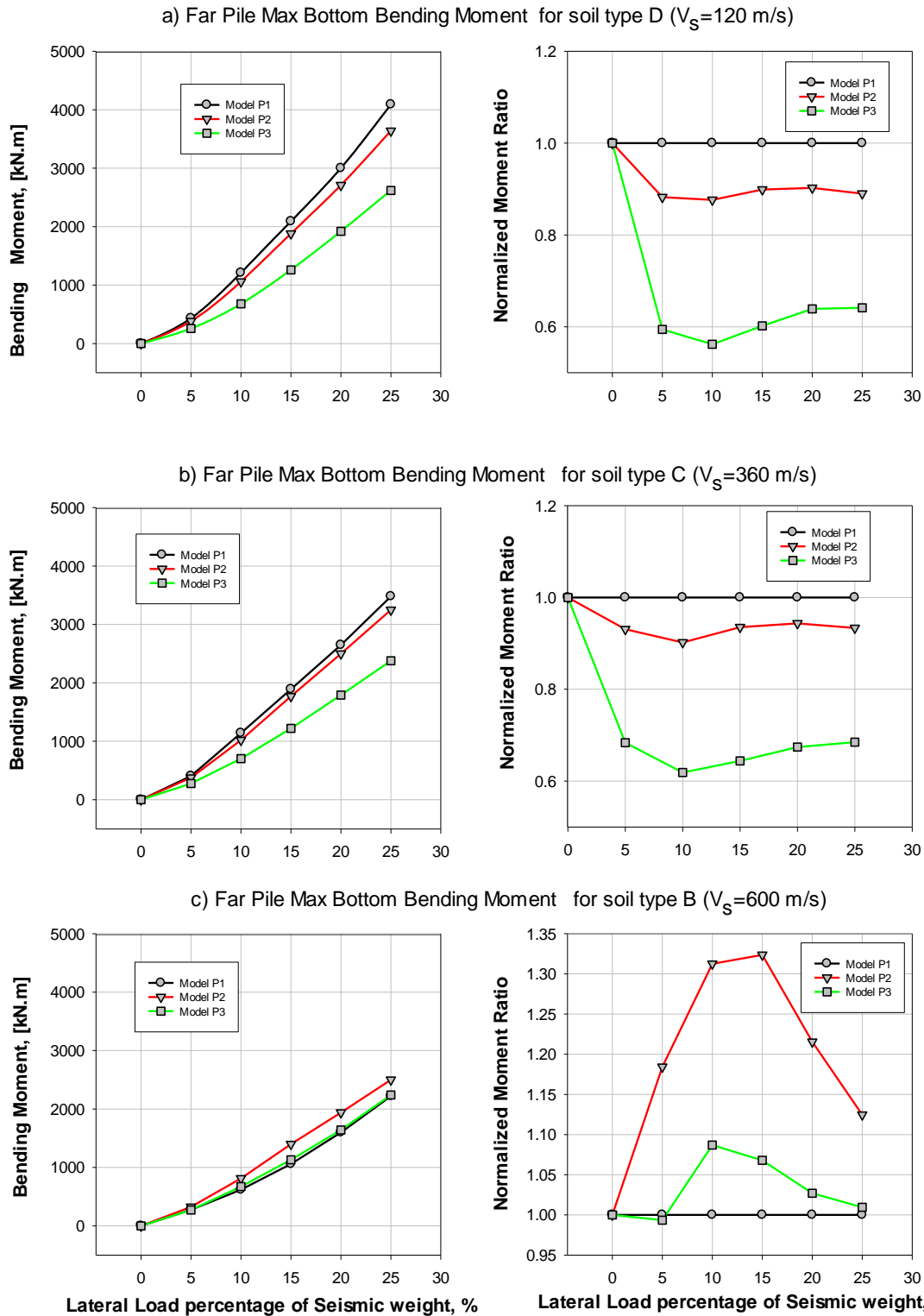


**Fig.14: Bottom Bending Moment of far piles systems left figure and Normalized with respect to profile P1- right figure versus lateral load coefficient
 a)for $V_s=120$ m/sec; b) for $V_s=360$ m/sec; c) for $V_s=600$ m/sec**



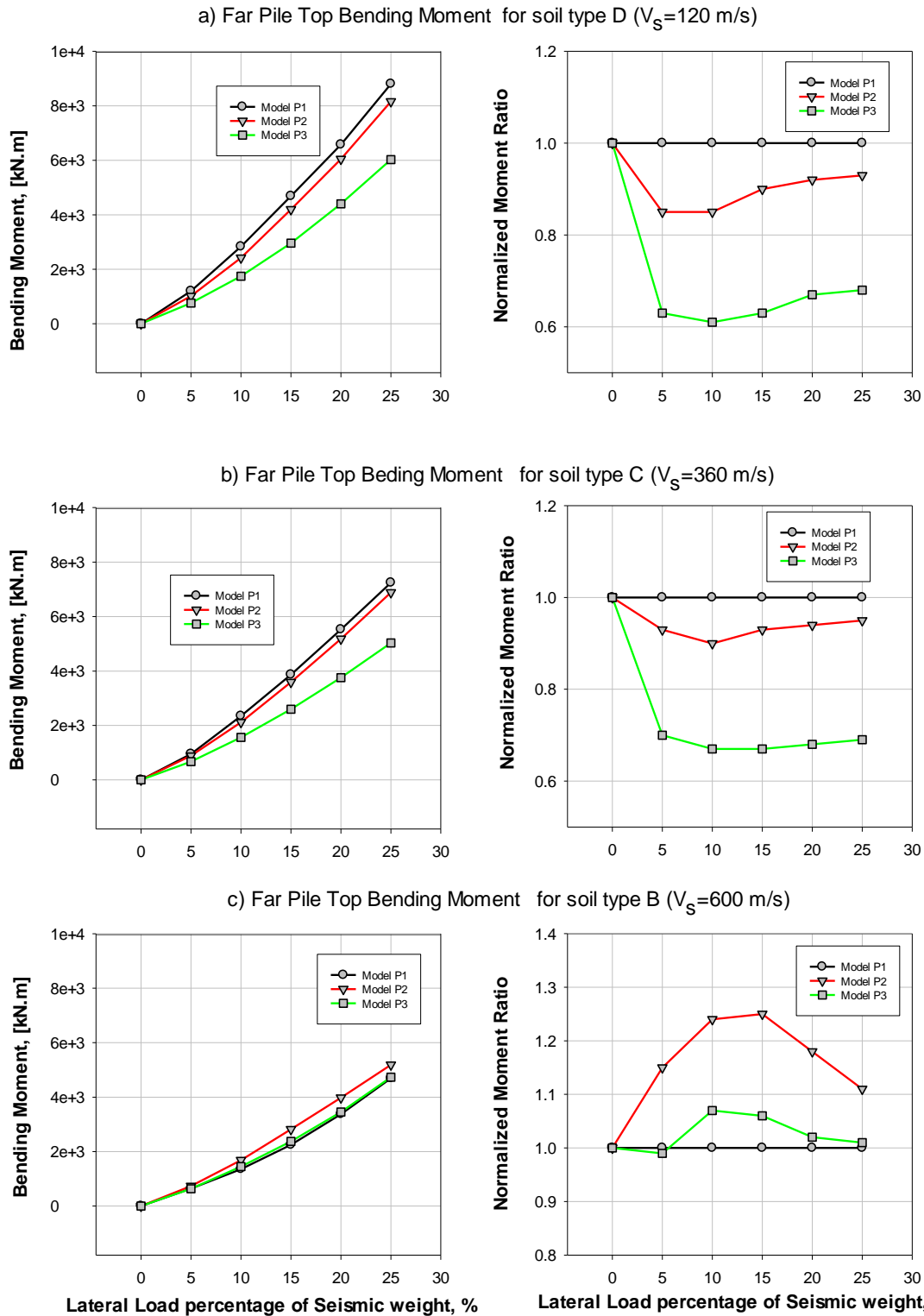


Fig.15: Top Bending Moment of far piles systems left figure and Normalized with respect to profile P1- right figure versus lateral load coefficient
a)for $V_s=120$ m/sec; b) for $V_s=360$ m/sec; c) for $V_s=600$ m/sec



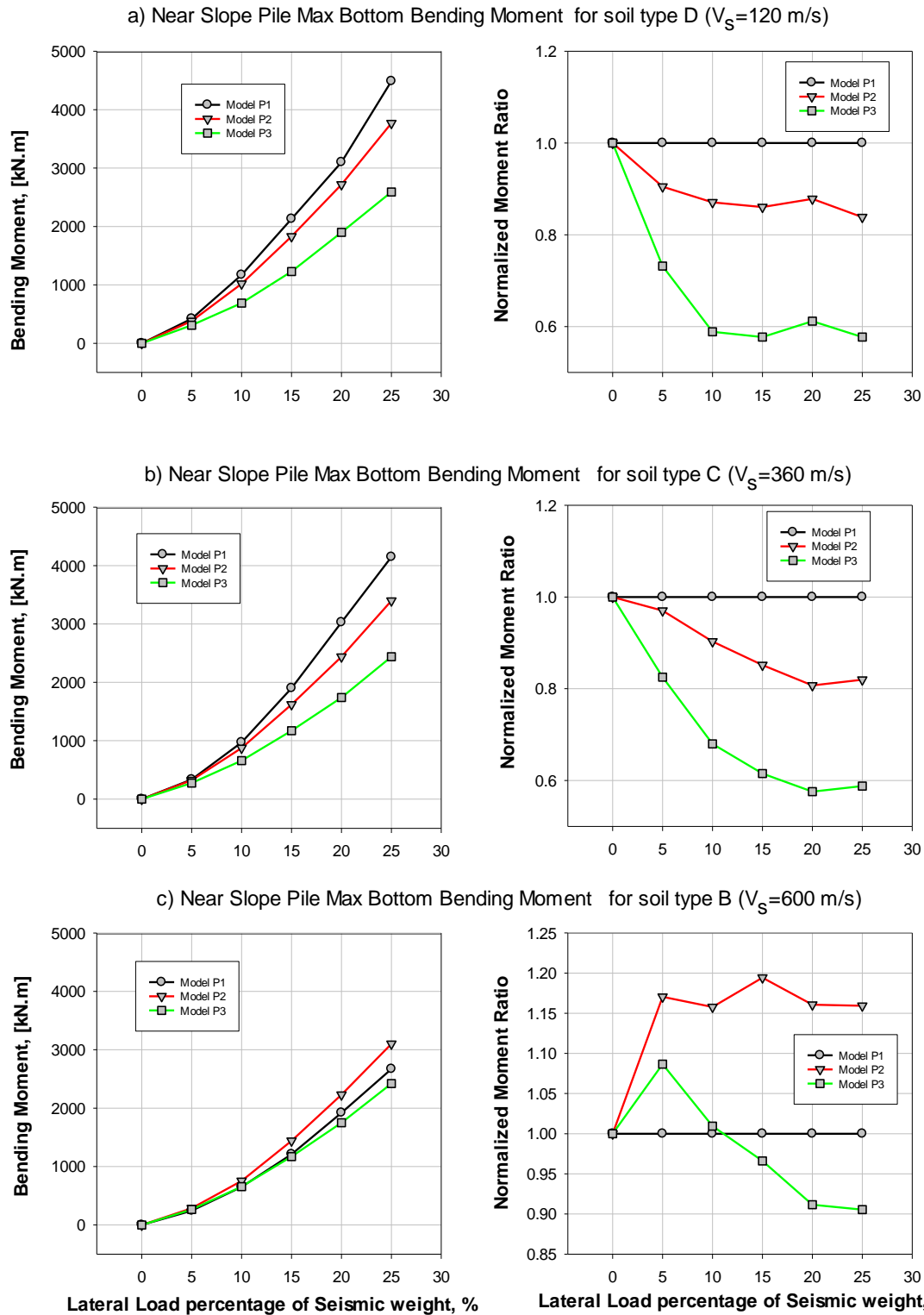


Fig.16: Bottom Bending Moment of near slope piles left figure and Normalized with respect to profile P1- right figure versus lateral load coefficient a)for $V_s=120$ m/sec; b) for $V_s=360$ m/sec; c) for $V_s=600$ m/sec



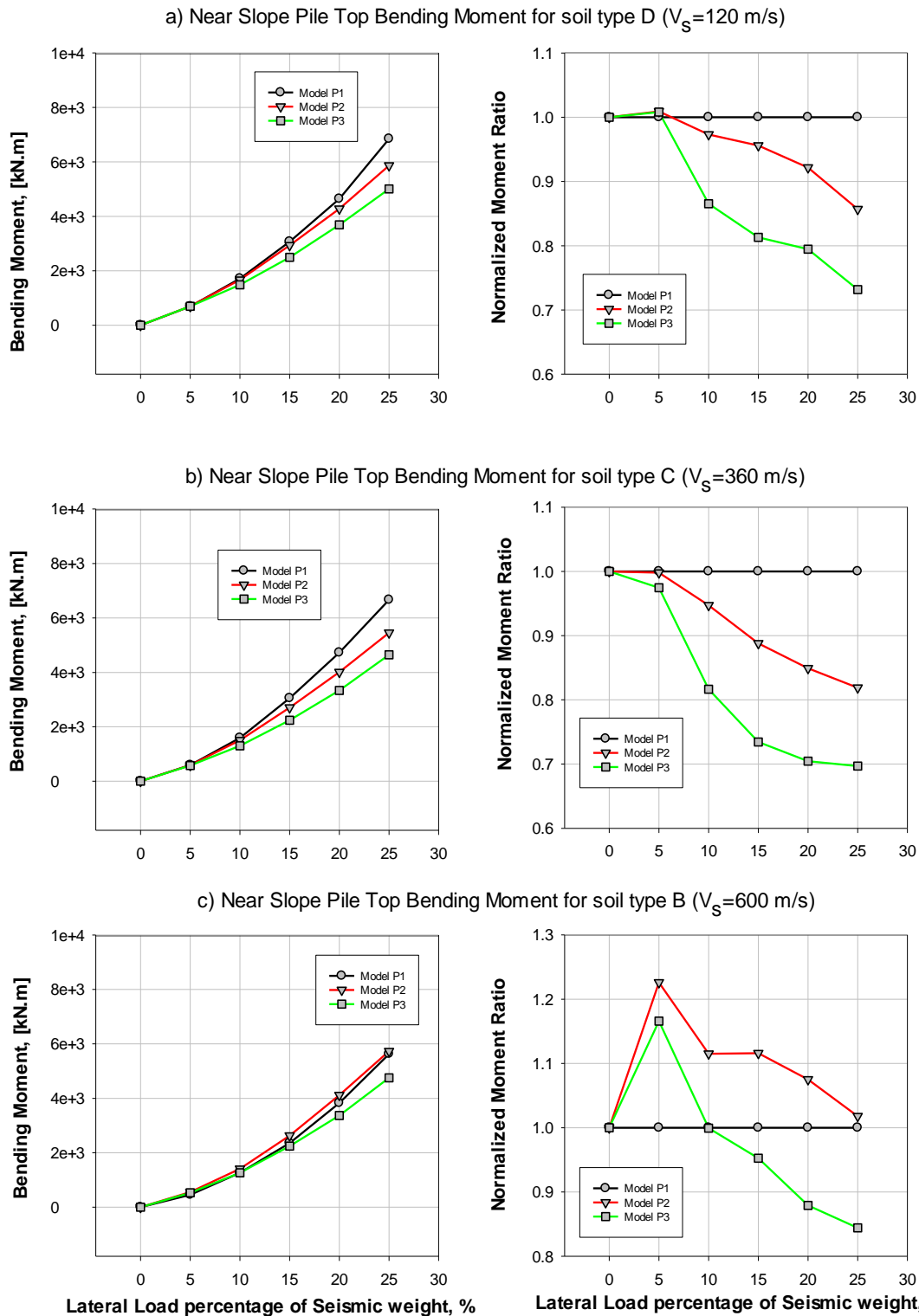


Fig.17: Top Bending Moment of near slope piles left figure and Normalized with respect to profile P1- right figure versus lateral load coefficient a)for $V_s=120$ m/sec; b) for $V_s=360$ m/sec; c) for $V_s=600$ m/sec



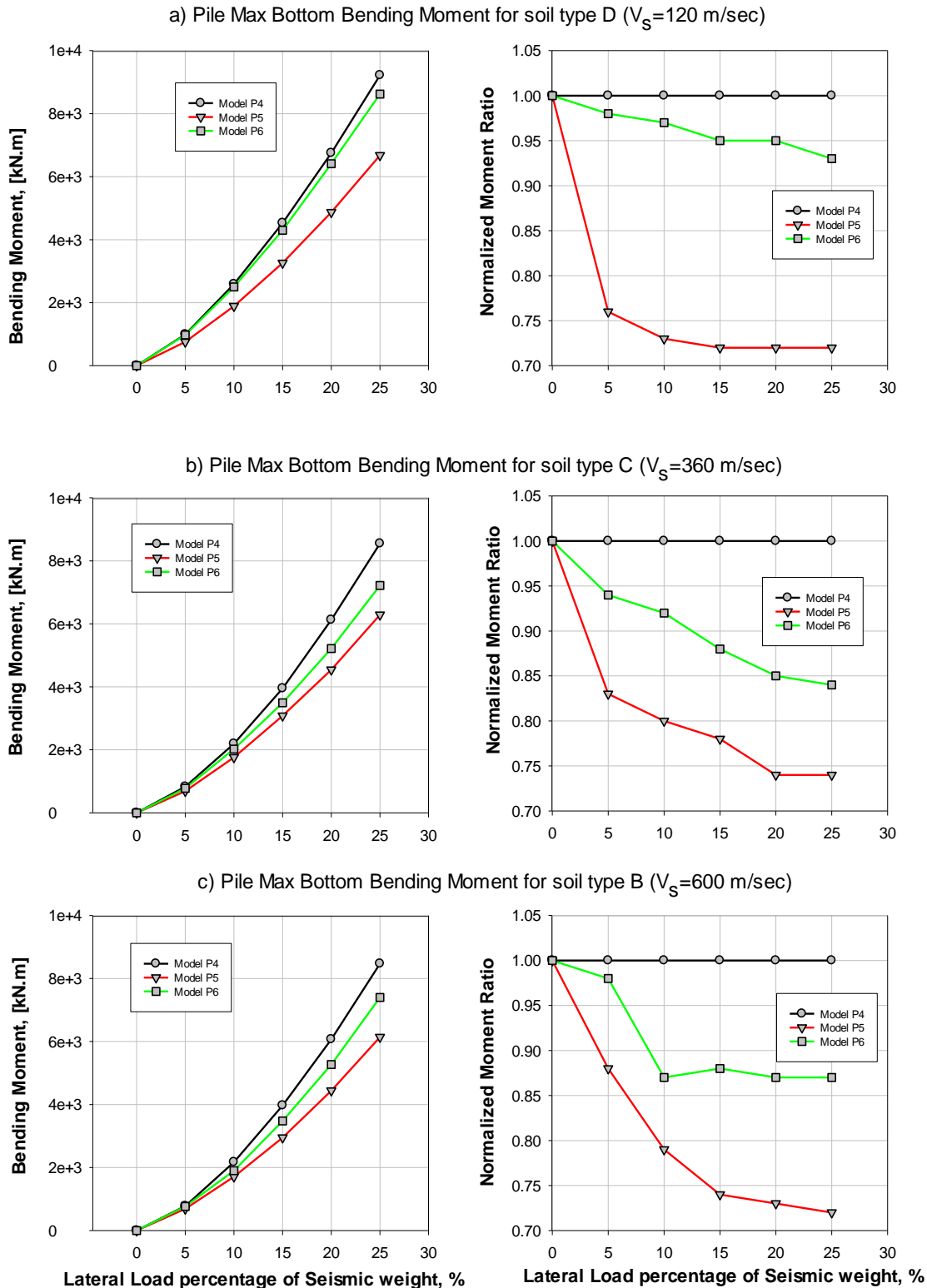


Fig.18: Bottom Bending Moment of single pile systems left figure and Normalized with respect to profile P4- right figure versus lateral load coefficient a)for Vs=120 m/sec; b) for Vs=360 m/sec; c) for Vs=600 m/sec

Conclusions

The influence of soil structure interaction on seismic response of laterally loaded piles at the slope of a

spill through bridge abutment is investigated. The objective is to assess the validity of present design codes which assumes the soil to cause only lateral



load "soil pressure" on the abutment, and ignores any presence of soil support. Results showed that ignoring the presence of soil support leads to uneconomical pile system design (overdesign) which causes unnecessary increases in construction cost. In particular, for the soil profiles and pile configuration considered, and limited to material properties and load levels assumed in this work:

For two rows of piles systems in soil type D, system P2 (slope 3:2 with terrace) has a drift that is between 85% and 90% of that of system P1 (slope 3:2 without terrace). Besides, system P3 (slope 3:1) has a drift that is about 50% of that of system P1. Similarly, the drift of the systems P2 and P3 in soil type C is shown to be 77% and 40% of system P1, respectively.

For single row of piles systems, the drift of system P6 (slope 3:2 with terrace) is about 65% to 80% of that of system P4 (slope 3:2 without terrace), depending on soil stiffness. Further, system P5 (slope 3:1) has a drift that is about 40% of that of system P4.

For two rows of piles systems and considering soil types C and D, top and bottom bending moments in systems P2(slope 3:2 with terrace) and P3 (slope 3:1) decrease up to 80% and 60% of that of system P1.

For single row of piles systems, bottom bending moments in systems P6 (slope 3:2 with terrace) and P5 (slope 3:1) decrease up to about 90% and 75% of that of system P4.

Depth of point of zero shear is also influenced by both soil stiffness and system profile. Systems with slope 3:2 with terrace has a depth of point of zero shear in the order of 85% of that of similar systems with slope 3:2 without terrace. Moreover, systems with slope 3:1 have depths of point of zero shear in the order of about 75% of that of systems with slope 3:2.

Committees of design codes both nationally and internationally are encouraged to modify their design methods of spill-through bridge abutment to include the support effects of soil.

References

- FLAC. Itasca, "Fast Lagrangian analysis of continua," Itasca Consulting Group Inc., Minneapolis, Minn, 2000.
- L. Chen and H. Poulos, "Approximation of lateral soil movements for analyzing lateral pile response," in Proc. 20th Annual Seminar of Geot. Divn., HK Inst. Engrs, 2001, pp. 14-23.
- S. Mezazigh and D. Levacher, "Laterally loaded piles in sand: slope effect on py reaction curves," Canadian Geotechnical Journal, vol. 35, no. 3, pp. 433-441, 1998.
- J. Wartman, R. B. Seed, and J. D. Bray, "Shaking table modeling of seismically induced deformations in slopes," Journal of Geotechnical and Geoenvironmental Engineering, vol. 131, no. 5, pp. 610-622, 2005.
- S. Prakash and S. Kumar, "Nonlinear lateral pile deflection prediction in sands," Journal of Geotechnical Engineering, [2311](#) vol. 122, no. 2, pp. 130-138, 1996.
- SEAOC Seismic design manual (2000), Structural Engineering Association of California.
- Kramer, S. L. (1996). Geotechnical earthquake engineering. Pearson Education India.

